

Side-chain conformational changes upon protein-protein association

Anatoly M. Ruvinsky^a, Tatsiana Kirys^{a,b}, Alexander V. Tuzikov^b, and Ilya A. Vakser^{a,c,1}

^aCenter for Bioinformatics, The University of Kansas, Lawrence, Kansas 66047

^bUnited Institute of Informatics Problems, National Academy of Sciences, 220012 Minsk, Belarus

^cDepartment of Molecular Biosciences, The University of Kansas, Lawrence, Kansas 66045

¹To whom correspondence should be addressed. E-mail: vakser@ku.edu

Text pages: 21, Figures: 6

Abstract

Conformational changes upon protein-protein association are the key element of the binding mechanism. The study presents a systematic large-scale analysis of such conformational changes in the side chains. The results indicate that short and long side chains have different propensities for the conformational changes. Long side chains with three or more dihedral angles are often subject to large conformational transition. Shorter residues with one or two dihedral angles typically undergo local conformational changes not leading to a conformational transition. The relationship between the local readjustments and the equilibrium fluctuations of a side chain around its unbound conformation is suggested. Most of the side chains undergo larger changes in the dihedral angle most distant from the backbone. The amino acids with symmetric aromatic (Phe and Tyr) and charged (Asp and Glu) groups show the opposite trend where the near-backbone dihedral angles change the most. The frequencies of the core-to-surface interface transitions of six nonpolar residues and Tyr exceed the frequencies of the opposite, surface-to-core transitions. The binding increases both polar and nonpolar interface areas. However, the increase of the nonpolar area is larger for all considered classes of protein complexes. The results suggest that the protein association perturbs the unbound interfaces to increase the hydrophobic forces. The results facilitate better understanding of the conformational changes in proteins and suggest directions for efficient conformational sampling in docking protocols.

Keywords: conformational changes, protein recognition, structure prediction, structural bioinformatics

Introduction

Protein structure-function relationships with the focus on conformational changes upon protein-protein association have been the subject of extensive research, including systematic studies on protein sets (1-7) and specific proteins (8-13). The theory of such conformational changes has been evolving from the early “lock-and-key” concept (14), through the induced-fit model (15), to the paradigm of the conformational selection (16-20). The knowledge and understanding of these conformational changes have been accumulated and implemented in algorithms for predicting the structure of protein complexes, as evidenced by the CAPRI experiment (21). Still the conformational changes upon the formation of a complex are one of the greatest challenges for researchers studying protein interactions. A direct way to tackle this problem is to study the differences between the unbound and the bound structures of the same protein (1, 2, 6) or the differences between the alternative conformations in unbound proteins (4, 5). An encouraging factor is the growth of the PDB (22), which has been the source for studies of the side-chain conformations in proteins in general (23-30). In the 90’s when only a few proteins had both bound and unbound structures known (31), Betts and Sternberg (2) studied 39 pairs of bound and unbound proteins, with only eight of the complexes having unbound structures of both binding proteins. Recently side-chain transitions were analyzed on a set of 124 protein complexes with known unbound structures (6). Currently, such sets (called docking benchmark sets because of their primary use in docking validation) contain a significantly larger and growing number of complexes (32, 33). Our DOCKGROUND non-redundant benchmark set (33) used in this study has 233 protein complexes, 99 of them having unbound structures of both binding proteins (134 complexes have unbound structure for one of the proteins).

Protein structures reveal a rich variety of conformational changes that occur at different scales upon binding (34). This includes domain motions, local folding-unfolding transitions, transitions between regular secondary structure elements in “chameleon sequences” (35, 36), disorder-to-order transitions (36, 37), and other changes in protein backbone and side chains. Although in general the different types of the conformational changes may be inter-related, in this study we focus on the conformational changes in the side chains. This choice is motivated by the fact that the majority of protein complexes in the non-redundant benchmark sets (32, 33) have small C^α RMSD between bound and unbound structures. Indeed, 71% of the DOCKGROUND set (33) used in this study has C^α RMSD < 2Å for 71% of the complexes. The Benchmark set from Weng’s group (32) has interface C^α RMSD < 2.2Å for 84% of complexes. Thus studying conformational changes in the side chains is important for the development of better protein-protein docking procedures (38-42). The focus on the side chains also follows the “divide-and-conquer” paradigm: elucidating the side-chain conformational changes first, then proceeding to the backbone flexibility, and eventually to their combination (planned for our future study).

Previous studies related to the side-chain conformational changes analyzed the dynamics of the changes (43-47). The scale of the conformational change was found to be determined to a significant extent by the residue’s surrounding (the environment effect). The effect appears as a decreased number of rotamers in the buried residues in comparison with the surface residues (43, 44, 46), as a small RMSD between bound and unbound states of pocket side chains (3), or as reduced fluctuations of the center of mass of such residues (48). The side-chain dynamics made it possible to differentiate the roles of the interface residues in binding, and develop a concept of anchor and latch residues that show restricted mobility and pass through similar conformations in molecular dynamics trajectories of the bound and unbound states (43, 47). The concept was

extended to include conserved residues at protein interfaces with similar properties (46). The influence of the conformational changes on the binding entropy has been studied (45). Guharoy et al (6) found that the interface residues undergo more significant conformational changes and often have higher energies than the other surface residues.

Our study presents an analysis of the conformational changes of the core and the surface side chains accompanying non-covalent protein heterodimerization. We show that the mechanism and the scale of the conformational changes depend on the side chain length and the proximity of the dihedral angle to the protein backbone. Long side chains, with three or more dihedral angles, are more often subject to large conformational transitions ($\sim 120^\circ$ of χ angle change). Shorter residues, with one or two dihedral angles, typically undergo small conformational changes ($\sim 40^\circ$) leading to local readjustments. We suggest that the local readjustments result from the equilibrium fluctuations of the side chain around its unbound conformation. The results show that about one tenth of the complexes in our study went through the local interface changes only. All other complexes are subject to the interplay of the large conformational transitions and the local readjustments. In most residues, the largest conformational changes occur in the dihedral angle most distant from the backbone. The opposite trend is found in the residues with symmetric aromatic (Phe and Tyr) and charged (Asp and Glu) groups, where the χ angle closest to the backbone changes most. The study also reveals the interface conformational changes leading to disorder-to-order transitions and changes of the residue surface area that result in core-to-surface and surface-to-core transitions.

Results and Discussion

Comparison of the dihedral angles values in bound and unbound residues was performed on the DOCKGROUND docking benchmark set containing the bound and unbound structures of same proteins (see Methods). The results (Fig. 1) reveal two trends: (1) generally the extent of the conformational changes increases with the increase of the number of dihedral angles in the side chain, and (2) the extent is larger for the surface interface residues than for the surface non-interface and the core residues. The relatively smaller conformational changes in the core can be explained by the tight packing. A number of the surface non-interface residues are part of the crystal packing interfaces. The relatively smaller conformational changes in the surface non-interface residues may suggest that the crystal packing interactions on average are weaker than interactions across the biological interfaces. However, the exact contribution of the crystal packing effect in the non-interface residues is beyond the scope of this study, which is focused on the analysis of the residues at the biological interfaces.

The results show that Pro, Cys and His have larger conformational changes on the non-interface surface than at the interface (Fig. 1). However, the increase is not statistically significant. The average RMSD of the interface residues with one, two, three, and four dihedral angles is 0.75, 1.22, 1.94 and 2.54Å, and the average root-square deviation of the dihedral angles (RSD, see Methods) is 40.5°, 55.1°, 111.3° and 135.0°, correspondingly. Since the dihedral angle tend to cluster near 180°, 60°, and -60° (the *trans*, *gauche*⁺, and *gauche*⁻ conformations), one can conclude that the side chains with one or two χ angles undergo local conformational changes, whereas the side chains with three or four χ angles can undergo a conformational transition between the energy minima. Moreover, since the average RSDs in the long side chains (the ones with more χ angles) vary around 120° (distance between two adjacent energy minima), one can

assume that the conformational transitions most likely occur in a single χ angle. Other dihedral angles in the long side chains as well as those in the short side chains typically undergo a local readjustment upon the binding. It is worth noting that all the long side chains are polar, except Met. Among the side chains with two and one χ angles, Asn, His and Ser, which show the largest average dihedral angle RSD in the group, are also polar. Three non-polar residues Cys, Pro and Phe, and polar Tyr have the smallest changes of dihedral angles. Cys and Pro are the least variable in terms of RMSD. One can assume that the difference in the degree of conformational changes of polar and nonpolar residues may result from different packing around these residues. The nonpolar residues have high propensity for the tightly packed protein core, whereas the polar residues often have exposed conformations that loosen their structural surrounding allowing more space for change.

The local readjustments of the short side chains likely occur due to the thermal fluctuations of dihedral angles. Since the thermal fluctuations deviate on average $\pm 20^\circ$ from the equilibrium (49), one can estimate the average χ angle RSD (Eq. 1) due to the thermal fluctuations as $\Delta\bar{\chi}^T \approx 40\sqrt{n}$. For the side chains with one or two χ angles ($n = 1$ or 2) we obtain $\Delta\bar{\chi}_1^T = 40^\circ$ and $\Delta\bar{\chi}_2^T = 56.6^\circ$ which are in excellent agreement with the statistically-derived average RSDs $\Delta\chi_1 = 40^\circ$ and $\Delta\chi_2 = 55.1^\circ$ (see above). The thermal fluctuations likely play a role of the “lock-and-key lubricant” providing plasticity of interfaces needed for the exact fit upon binding. The average RSDs $\Delta\chi_3 = 111.3^\circ$ and $\Delta\chi_4 = 135.0^\circ$ in the longer side chains deviate from the fluctuations-based estimates $\Delta\bar{\chi}_3^T = 69.3^\circ$ and $\Delta\bar{\chi}_4^T = 80^\circ$. The deviations increase with the increase of the number of the χ angles from 2 to 4. The increase of the deviations may be explained by the ability of the longer residues to establish interactions across interface earlier than the shorter residues. Indeed, binding proteins “optimize” conformations of the long residues

at the early stages of their approach. The short residues get involved at later stages of binding, and thus have less time for conformational sampling. The increase of the deviations also points toward a greater role of the induced fit mechanism in comparison to the “lubricated lock-and-key” mechanism for the longer side chains. The results show that the “lubricated lock-and-key” mechanism only is present in 11% of the complexes in the set. The rest 89% of the complexes are subject to the interplay of both the induced fit and the “lubricated fit” mechanisms. 66% of the complexes reveal 1 to 4 conformational transitions per interface, which on average consists of 18 residues.

The share of the conformational transitions, defined as conformational changes $\geq 100^\circ$ in one of χ angles, among all the conformational changes is larger for the side chains with three or four χ than for the side chains with one or two χ (Fig. 2). The conformational transitions at the interface occur more frequently than on the non-binding surface and in the core. This observation is in agreement with the results of Guharoy et al (6) obtained on a smaller set of complexes using different definitions of surface and interface. The data in Fig. 2 show that only His residue has a higher frequency of the conformational transitions on the non-binding surface. Thr, Cys, Ile, Asn and Phe have similar frequencies of the interface and non-interface surface conformational transitions. The probability of the interface transitions $> 100^\circ$ simultaneously in several dihedral angles decreases significantly with the increase of the number of the dihedral angles. The dihedral angle change associated with the rotation of a symmetric group in Asp, Phe, Tyr and Glu cannot exceed 90° ; thus these residues do not undergo conformational transitions simultaneously in all χ angles (Fig. 2).

To further detail the picture, we computed average changes of each χ angle in the amino acids (Fig. 3). Six of the nine side chains with two dihedral angles have larger changes of the

outer angle (χ_2) in comparison with the near-backbone angle (χ_1). The same trend is observed for all the side chains with three and four χ angles with the exception of Glu, which is slightly more prone to the changes in the first and second χ angles. Two amino-acid side chains with aromatic groups (Phe and Tyr) and two charged amino acids (Asp and Glu) demonstrate an opposite trend where the outer χ changes less than the near-backbone one. This trend is explained partly by the reduced interval of variability of the outer χ due to the symmetry of the amino acid's terminal groups.

In agreement with earlier studies (36, 37, 50) the results indicate that binding can decrease structural disorder at protein interfaces. Four percent (164 residues) of all interface residues in the set exhibited disorder-to-order transition upon binding. The disordered residues were defined as those with missing coordinates in the crystal structure. Most of the disordered residues (39%) were Ala, Gly, Glu, or Thr. On the other hand, only 11% of the disordered residues were Cys, His, Phe, Ile, Pro, Trp, or Tyr. This observation is in agreement with the classification of amino acids into order-promoting and disorder-promoting ones (37) and correlates well with the amino acids' ability to fluctuate (48).

An important conformational aspect of protein association is the changes of the residue surface area upon binding. The rate of the core-to-surface interface transitions (Fig.4), calculated as a percentage of all transitions, varied from 10-11% (Tyr, Val, and Phe) to 4% (Asn, Glu and Lys). Examples of the core-to-surface interface transitions are shown in Fig. 5 and 6. The rate of the surface-to-core interface transitions varies from 2% (Pro) to 8% (Met). Interestingly, on average, the rate of the core-to-surface transitions exceeds that of the surface-to-core transitions for all amino acids, except Asn. The largest difference between the rates is observed in six nonpolar residues, Ala, Val, Pro, Ile, Leu, Phe, and a polar Tyr. At protein interfaces, Tyr often

has been identified as a hot spot (51). The bias in the core-to-surface transitions towards the nonpolar residues suggests that protein-protein interactions may perturb an unbound interface to increase the nonpolar interface area, thus increasing the hydrophobic contribution to the binding free energy (a major force stabilizing protein complexes). To test this hypothesis, we calculated average changes of polar and nonpolar interface areas induced by binding. On average, the binding increases both the polar and nonpolar interface areas in the complex. However, the increase of the nonpolar area is greater for all classes of complexes:

$$\Delta S_p = 17.4 \pm 7.5 \text{ \AA}^2 \text{ and } \Delta S_n = 38.3 \pm 17.2 \text{ \AA}^2 \text{ for antibody/antigen;}$$

$$\Delta S_p = 25.9 \pm 7.8 \text{ \AA}^2 \text{ and } \Delta S_n = 32.9 \pm 12.8 \text{ \AA}^2 \text{ for enzyme/inhibitor; and}$$

$\Delta S_p = 12.9 \pm 6.1 \text{ \AA}^2$ and $\Delta S_n = 24.2 \pm 9.7 \text{ \AA}^2$ for other ($\Delta S_{n,p}$ is the change of the nonpolar or polar interface area).

Two typical scenarios of the core-to-surface transitions were observed, as illustrated in Fig. 5 and 6. In the first scenario, a core side chain does not change conformation, but other residues in the vicinity change conformations to increase the side-chain surface (e.g., Phe41 and Lys224 in Fig. 5 and Leu102, Pro107 and Met129 in Fig. 6). In the second scenario, both the side chain and its neighbors change their conformations (e.g., Leu99 in Fig. 5). A case where a core side chain undergoes a conformational change and its structural neighbors within 5Å stay unchanged was not observed.

Conclusions

Knowledge of the conformational changes upon protein binding is essential for understanding molecular mechanisms of life processes and our ability to model cell phenomena. The study focuses on the side-chain conformational changes in protein heterodimerization. The results

indicate that short and long side chains have propensities for different mechanisms of the conformational changes. Long side chains with three or more dihedral angles are often subject to the induced fit mechanism resulting in a conformational transition. Shorter residues with one or two dihedral angles typically undergo local conformational changes not leading to a conformational transition. The relationship between the local readjustments and the equilibrium fluctuations of a side chain around its unbound conformation is suggested. The local readjustments were dominant in 11% of the complexes. All other complexes were subject to the interplay of the induced fit and the local readjustments. We showed that most of the side chains undergo larger changes in the dihedral angle most distant from the backbone. The amino acids with symmetric aromatic (Phe and Tyr) and charged (Asp and Glu) groups show the opposite trend where the near-backbone dihedral angles change the most. The frequencies of the core-to-surface interface transitions of six nonpolar residues and Tyr exceed the frequencies of the inverse, surface-to-core transitions. The binding increases both the polar and nonpolar interface areas. However, the increase of the nonpolar area is larger for all considered classes of the protein complexes. These findings suggest that the protein association perturbs the unbound interfaces to increase the hydrophobic forces. The results facilitate better understanding of the conformational changes in proteins and suggest directions for more efficient conformational sampling in docking protocols.

Methods

The results are obtained on a non-redundant benchmark set of 233 non-obligate protein-protein complexes from the DOCKGROUND resource <http://dockground.bioinformatics.ku.edu> (33, 52). The set contains unbound structures of both proteins for 99 complexes and the unbound structure

of one of the proteins for 134 complexes. The structures were selected from PDB based on the following criteria: sequence identity between bound and unbound structures > 97%, sequence identity between complexes < 30%, homomultimers and crystal packing complexes excluded.

Conformational changes between unbound and bound conformations were considered for each of the protein side chains in the set. The conformational changes were expressed in terms of the root mean square deviation (RMSD) of the atoms coordinates and the root square deviation (RSD) of the dihedral angles

$$\Delta\chi = \left[\sum_{i=1}^n D_i^2(\chi_i^b, \chi_i^u) \right]^{1/2}, \quad (1)$$

where n is the number of the dihedral angles in a side chain, i is the index of a dihedral angle χ_i , b and u indicate bound and unbound conformations. Function

$$D_i(\chi_i^b, \chi_i^u) = \begin{cases} |\chi_i^b - \chi_i^u|, & \text{if } |\chi_i^b - \chi_i^u| \leq 180^\circ \\ 360^\circ - |\chi_i^b - \chi_i^u|, & \text{if } |\chi_i^b - \chi_i^u| > 180^\circ \end{cases} \quad (2)$$

gives the shortest distance between the dihedral angles on the circle. The values of the dihedral angles were taken from 0° to 360° , except the last angles in Phe, Tyr, Asp and Glu, which were taken from 0° to 180° due to the symmetry of aromatic and charged groups (53). The dihedral angles analyzed for Arg were χ_{1-4} , because the tip of the side chain containing χ_5 is planar. The dihedral angles were determined using Dang program <http://kinemage.biochem.duke.edu/software/dang.php>. The conformational changes were placed in eighteen groups corresponding to standard amino acids (Gly and Ala were not considered). The average conformational changes and the standard deviations were computed for the interface residues (surface residues at protein interfaces), non-interface surface residues, and core residues. Surface residues were defined as those with the relative solvent accessible surface area (RASA) > 25%, as determined by

NACCESS (54). Interface residues were defined as those losing $> 1\text{\AA}$ of their surface upon binding (46).

Acknowledgments

The study was supported by R01 GM074255 grant from NIH. We thank Dr. Simon C. Lovell for the code converting dihedral angles into Cartesian coordinates of the atoms.

References

1. Lo Conte L, Chothia C, & Janin J (1999) The atomic structure of protein-protein recognition sites. *J. Mol. Biol.* 285:2177-2198.
2. Betts MJ & Sternberg MJE (1999) An analysis of conformational changes on protein-protein association: Implications for predictive docking. *Protein Eng.* 12:271-283.
3. Li X, Keskin O, Ma B, Nussinov R, & Liang J (2004) Protein-protein interactions: Hot spots and structurally conserved residues often locate in complemented pockets that pre-organized in the unbound states: Implications for docking. *J. Mol. Biol.* 344:781-795.
4. Davis IW, Arendall WB, Richardson DC, & Richardson JS (2006) The backrub motion: How protein backbone shrugs when a sidechain dances. *Structure* 14:265-274.
5. Bhardwaj N & Gerstein M (2009) Relating protein conformational changes to packing efficiency and disorder. *Protein Sci.* 18:1230-1240.
6. Guharoy M, Janin J, & Robert CH (2010) Side-chain rotamer transitions at protein-protein interfaces. *Proteins* 78:3219-3225.
7. Kidd BA, Baker D, & Thomas WE (2009) Computation of conformational coupling in allosteric proteins. *PLoS Comp. Biol.* e1000484.
8. Clackson T & Wells JA (1995) A hot spot of binding energy in a hormone-receptor interface. *Science* 267:383-386.
9. Wlodarski T & Zagrovic B (2009) Conformational selection and induced fit mechanism underlie specificity in noncovalent interactions with ubiquitin. *Proc. Natl. Acad. Sci. USA* 106:19346-19351.

10. Eisenmesser EZ, Millet O, Labeikovsky W, Korzhnev DM, Wolf-Watz M, Bosco DA, Skalicky JJ, Kay LE, ., & Kern D (2005) Intrinsic dynamics of an enzyme underlies catalysis. *Nature* 438:117-121.
11. Zhang XJ, Wozniak JA, & Matthews BW (1995) Protein flexibility and adaptability seen in 25 crystal forms of T4 lysozyme. *J. Mol. Biol.* 250:527-552.
12. Bui JM, Radic Z, Taylor P, & McCammon JA (2006) Conformational transitions in protein-protein association: Binding of fasciculin-2 to acetylcholinesterase. *Biophys. J.* 90:3280-3287.
13. Lange OF, Lakomek NA, Fares C, Schroder GF, Walter KFA, Becker S, Meiler J, Grubmuller H, Griesinger C, & de Groot BL (2008) Recognition dynamics up to microseconds revealed from an RDC-derived ubiquitin ensemble in solution. *Science* 320:1471-1475.
14. Fischer E (1894) Einfluss der Configuration auf die Wirkung der Enzyme. *Ber. Dt. Chem. Ges.* 27:2985–2993.
15. Koshland DE (1959) Enzyme flexibility and enzyme action. *J. Cellular Compar. Physiol.* 54:245-258.
16. Changeux JP & Edelstein SJ (2005) Allosteric mechanisms of signal transduction. *Science* 308:1424-1428.
17. Bosshard HR (2001) Molecular recognition by induced fit: How fit is the concept? *News Physiol. Sci.* 16:171-173.
18. Boehr DD & Wright PE (2008) How do proteins interact? *Science* 320:1429-1430.

19. Csermely P, Palotai R, & Nussinov R (2010) Induced fit, conformational selection and independent dynamic segments: An extended view of binding events. *Trends Biochem. Sci.* 35:539-546.
20. Zhou HX (2010) From induced fit to conformational selection: A continuum of binding mechanism controlled by the timescale of conformational transitions. *Biophys. J.* 98:L15–L17.
21. Janin J, Henrick K, Moult J, Ten Eyck L, Sternberg MJE, Vajda S, Vakser I, & Wodak SJ (2003) CAPRI: A Critical Assessment of PRedicted Interactions. *Proteins* 52:2-9.
22. Berman H, Henrick K, & Nakamura H (2003) Announcing the worldwide Protein Data Bank. *Nature Struct Biol.* 10:980.
23. Levitt M (1978) Conformational preferences of amino acids in globular proteins. *Biochemistry* 17:4277-4285.
24. Janin J & Wodak S (1978) Conformation of amino acid side-chains in proteins. *J. Mol. Biol.* 125:357-386.
25. Dunbrack RL & Cohen FE (1997) Bayesian statistical analysis of protein side-chain rotamer preferences. *Protein Sci.* 6:1661-1681.
26. Bromberg S & Dill KA (1994) Side-chain entropy and packing in proteins. *Protein Sci.* 3:997-1009.
27. Schrauber H, Eisenhaber F, & Argos P (1993) Rotamers: to be or not to be? An analysis of amino acid side-chain conformations in globular proteins. *J. Mol. Biol.* 230:592-612.
28. Lovell SC, Word JM, Richardson JS, & Richardson DC (2000) The penultimate rotamer library. *Proteins* 40:389-408.

29. Nayeem A & Scheraga HA (1994) A statistical analysis of side-chain conformations in proteins: Comparison with ECEPP predictions. *J. Protein Chem.* 13:283-296.
30. Ponder JW & Richards FM (1987) in *Cold Spring Harbor Symposia on Quantitative Biology* (Cold Spring Harbor Laboratory), pp. 421-428.
31. Jones S & Thornton JM (1996) Principles of protein-protein interactions. *Proc. Natl. Acad. Sci. USA* 93:13-20.
32. Hwang H, Pierce B, Mintseris J, Janin J, & Weng Z (2008) Protein-protein docking benchmark version 3.0. *Proteins* 73:705-709.
33. Gao Y, Douguet D, Tovchigrechko A, & Vakser IA (2007) DOCKGROUND system of databases for protein recognition studies: Unbound structures for docking. *Proteins* 69:845-851.
34. Goh CS, Milburn D, & Gerstein M (2004) Conformational changes associated with protein-protein interactions. *Curr. Opin. Struct. Biol.* 14:104-109.
35. Mezei M (1998) Chameleon sequences in the PDB. *Protein Eng.* 14:411-414.
36. Dyson HJ & Wright PE (2002) Coupling of folding and binding for unstructured proteins. *Curr. Opin. Struct. Biol.* 12:54-60.
37. Dunker AK, Lawson JD, Brown CJ, Williams RM, Romero P, Oh JS, Oldfield CJ, Campen AM, Ratliff CM, Hipps KW, *et al.* (2001) Intrinsically disordered proteins. *J. Mol. Graph. Mod.* 19:26-59.
38. Gray JJ (2006) High-resolution protein-protein docking. *Curr. Opin. Struct. Biol.* 16:183-193.
39. Andrusier N, Mashiach E, Nussinov R, & Wolfson HJ (2008) Principles of flexible protein-protein docking. *Proteins* 73:271-289.

40. Ritchie DW (2008) Recent progress and future directions in protein-protein docking. *Curr. Protein Peptide Sci.* 9:1-15.
41. Camacho CJ & Vajda S (2002) Protein-protein association kinetics and protein docking. *Curr. Opin. Struct. Biol.* 12:36-40.
42. Bonvin AMJJ (2006) Flexible protein-protein docking. *Curr. Opin. Struct. Biol.* 16:194-200.
43. Rajamani D, Thiel S, Vajda S, & Camacho CJ (2004) Anchor residues in protein-protein interactions. *Proc. Natl. Acad. Sci. USA* 101:11287-11292.
44. Smith GR, Sternberg MJE, & Bates PA (2005) The relationship between the flexibility of proteins and their conformational states on forming protein-protein complexes with an application to protein-protein docking *J. Mol. Biol.* 347:1077-1101
45. Grunberg R, Nilges M, & Leckner J (2006) Flexibility and conformational entropy in protein-protein binding. *Structure* 14:683-693.
46. Yagurtcu ON, Erdemli SB, Nussinov R, Turkay M, & Keskin O (2008) Restricted mobility of conserved residues in protein-protein interfaces in molecular simulations. *Biophys. J.* 94:3475-3485.
47. Kimura SR, Brower RC, Vajda S, & Camacho CJ (2001) Dynamical view of the positions of key side chains in protein-protein recognition. *Biophys. J.* 80:635-642.
48. Ruvinsky AM & Vakser IA (2010) Sequence composition and environment effects on residue fluctuations in protein structures. *J. Chem. Phys.* accepted.
49. Finkelstein AV & Ptitsyn OB (2002) *Protein Physics—A Course of Lectures* (Academic Press).

50. Fong JH, Shoemaker BA, Garbuzynskiy SO, Lobanov MY, Galzitskaya OV, & Panchenko AR (2009) Intrinsic disorder in protein interactions: Insights from a comprehensive structural analysis. *PLoS Comp. Biol.* 5:e1000316.
51. Bogan AA & Thorn KS (1998) Anatomy of hot spots in protein interfaces. *J. Mol. Biol.* 280:1-9.
52. Douguet D, Chen HC, Tovchigrechko A, & Vakser IA (2006) DOCKGROUND resource for studying protein-protein interfaces. *Bioinformatics* 22:2612–2618.
53. Dunbrack RL & Karplus M (1993) Backbone-dependent rotamer library for proteins: Application to side-chain prediction. *J. Mol. Biol.* 230:543-574.
54. Hubbard SJ & Thornton JM (1993) NACCESS. *Computer Program, Department of Biochemistry and Molecular Biology, University College London*
55. Song HK & Suh SW (1998) Kunitz-type soybean trypsin inhibitor revisited: Refined structure of its complex with porcine trypsin reveals an insight into the interaction between a homologous inhibitor from *Erythrina caffra* and tissue-type plasminogen activator. *J. Mol. Biol.* 275:347-363.
56. Transue TR, Gabel SA, & London RE (2006) NMR and crystallographic characterization of adventitious borate binding by trypsin. *Bioconjugate Chem.* 17:300-308.
57. Lim D, Park HU, De Castro L, Kang SG, Lee HS, Jensen S, Lee KJ, & Strynadka NC (2001) Crystal structure and kinetic analysis of beta-lactamase inhibitor protein-II in complex with TEM-1 beta-lactamase. *Nature Struct Biol.* 8:848-852.
58. Minasov G, Wang X, & Shoichet BK (2002) An ultrahigh resolution structure of TEM-1 beta-lactamase suggests a role for Glu166 as the general base in acylation. *J. Amer. Chem. Soc.* 124:5333-5340.

Figure Legends

Figure 1. Average conformational change between unbound and bound residues. (A) Change in Cartesian coordinates (RMSD), and (B) change in dihedral angles (RSD, see Methods). The residues are sorted left to right according to the increasing number of χ angles, and increasing mass (if the number of χ is the same). Standard deviation is shown for the interface residues.

Figure 2. The share of conformational transitions. The conformational transitions are defined as those with $\Delta\chi \geq 100^\circ$ in any of the dihedral angles. (A) Percentage of conformational transitions in all conformational changes between unbound and bound structures. (B) Percentage of simultaneous conformational transitions in one (light gray), two (dark gray), and three (black) χ angles for interface residues. The percentage for four χ angles is negligible (not shown). The percentage of conformational changes $<100^\circ$ in each dihedral angle is shown by open bars.

Figure 3. Average dihedral angle change for different structure regions. The change between unbound and bound conformers is shown for the core (+), non-interface surface (∇) and interface (#) residues. Standard deviation is shown for the interface residues.

Figure 4. Frequencies of transitions between surface and core at the interface.

Figure 5. Core-to-surface interface transitions in porcine pancreatic trypsin induced by soybean trypsin inhibitor. The bound structure is in magenta, and the unbound one is in blue. The bound/complex structure is 1avw (55) and the unbound trypsin structure is 2a31 (56). Phe41

keeps its conformation, while undergoing a core-to-surface transition with the relative solvent accessible surface area (RASA) change from 16.9% in the unbound state to 28.6% in the bound state, due to the conformational change in Lys60, which has two alternative unbound conformations. Lys224 keeps its conformation, while increasing its RASA from 24.1% to 28.2% due to the conformational change in Tyr217 (Δ RASA= 14.3%). Leu99 changes RASA from 19.9% to 34.4% due to its own conformational change and the change in Asn97 (Δ RASA=16.2%).

Figure 6. Core-to-surface interface transitions in TEM-1 β -lactamase induced by β -lactamase inhibitor protein-II. The bound structure is in magenta, and the unbound one is in blue. The bound/complex structure is 1jtd (57) and the unbound TEM-1 is 1m40 (58). Leu102 keeps its conformation, while undergoing core-to-surface transition with RASA change from 18.6% in the unbound state to 30% in the bound state, due to the conformational change in Gln99, which has two alternative unbound conformations. Pro107 keeps its conformation, while changing RASA from 22.3% to 34.1% due to the conformational changes in Tyr105 (Δ RASA=49.9%) and Lys111, which has two alternative unbound conformations. Met129 keeps its conformation, but changes RASA from 17.4% to 44.7% due to the conformational changes in Tyr105 and Lys215, which has two alternative unbound conformations. Glu104 changes RASA by 30.3%.

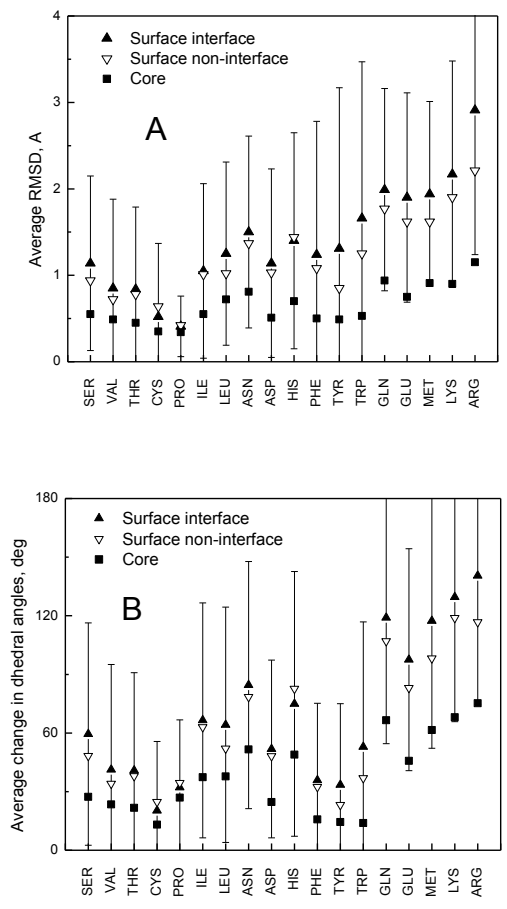


Figure 1

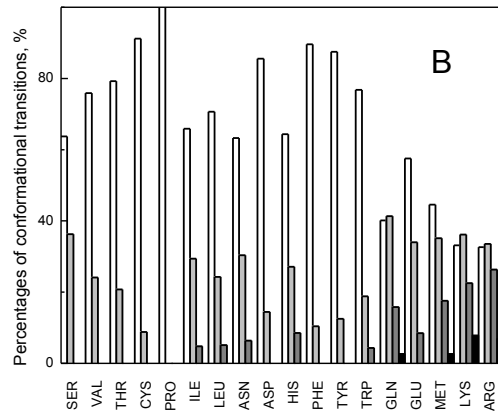
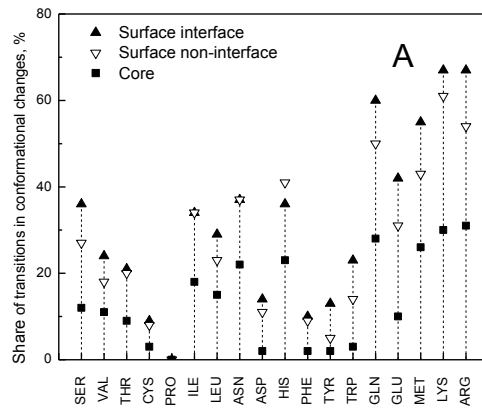


Figure 2

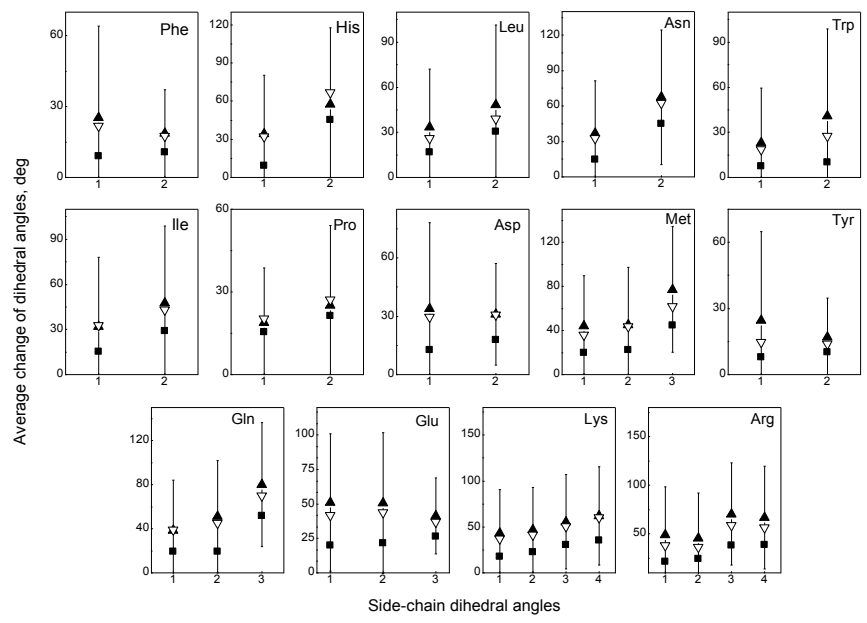


Figure 3

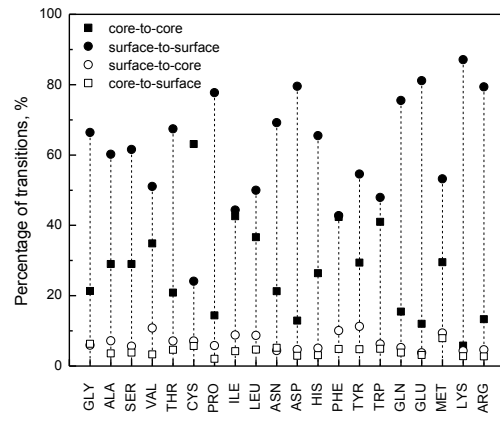


Figure 4

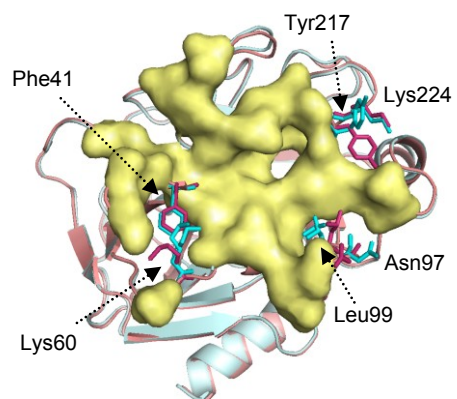


Figure 5

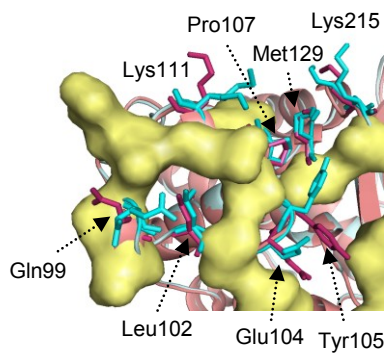


Figure 6